Fourth International Conference on Sustainable Construction Materials and Technologies
http://www.claisse.info/Proceedings.htm

SCMT4
Las Vegas, USA, August 7-11, 2016

Resistance to Chloride Penetration of Self-Healing Concrete with Encapsulated Polyurethane

Bjorn Van Belleghem*[1,2a], Philip Van den Heedeand[1, 2b], and Nele De Belie[1c]

*[1]Magnel Laboratory for Concrete Research, Department of Structural Engineering, Faculty of Engineering and Architecture, Ghent University, Technologiepark 904, BE-9052 Zwijnaarde, BELGIUM. [2]Strategic Initiative Materials (SIM vzw), project ISHECO within the program 'SHE', SIM vzw, Technologiepark 935, BE-9052 Zwijnaarde, BELGIUM.. [*1,2a]Email: <bjorn.vanbelleghem@ugent.be>, [*1,2b]Email: <philip.vandenheede@ugent.be>, [1c]Email: <nele.debelie@ugent.be>*

ABSTRACT

Reinforcement corrosion induced by diffusion of chlorides is one of the most important damage mechanisms that leads to the deterioration of reinforced concrete structures. Cracking of reinforced concrete structures during their service life is almost inevitable. Cracks form preferential pathways for the ingress of chlorides and will accelerate the onset of corrosion and its propagation. In this paper, autonomous self-healing of cracks by encapsulated polyurethane is investigated as a possible method to heal cracks and reduce chloride ingress through cracks without human intervention. Cracks in concrete specimens were created in two ways: by means of thin metal plates to create standardized artificial cracks and by means of splitting tests to create realistic cracks. A crack width of 0.3 mm was chosen since most design codes limit the crack width to that value. The resistance to chloride penetration of autonomously healed concrete was evaluated by the diffusion test as described in NT Build 443. Uncracked, cracked and healed specimens were subjected to a 165 g/l NaCl solution for 7 weeks. After that period chloride profiles in the crack region and in an area further away from the crack were obtained by potentiometric titrations. From the resulting chloride profiles it was concluded that the polyurethane was very well able to seal both artificial and realistic cracks and reduce the chloride content in the crack zone significantly. At depths below the surface larger than 14 mm, healing was able to reduce the total chloride content in the crack zone by more than 70%.

INTRODUCTION

Penetration of chlorides in reinforced concrete structures can lead to major durability problems. Chloride ions penetrating the concrete and reaching the steel reinforcement initiate corrosion which leads to degradation of the concrete structure. Cracking of reinforced concrete is an inevitable phenomenon which causes preferential pathways for chlorides to penetrate the concrete. This may lead to a very high local chloride concentration at the reinforcement. When this chloride concentration reaches a critical threshold value, corrosion will be initiated. Many studies with different test setups have been used to evaluate the

critical chloride content in reinforced concrete. However, reported results scatter over a large range. Angst et al. [2009] presented a review on the concept of the critical chloride content, stating that reported values in literature vary from 0.1 to 1.96 m%/binder. A recent study on the critical chloride content in fly ash concrete reported critical chloride ion concentrations of 1.58 to 1.78 m%/binder [Sun et al. 2015].

The influence of cracks on the chloride ingress in concrete has already been investigated in several studies. In most of these researches migration tests were used for the evaluation of chloride penetration. Jacobsen et al. [1996] were one of the first to investigate the effect of cracks on the transport of chlorides by means of a steady-state migration test. Djerbi et al. [2008] and Jang et al. [2011] also used steady-state migration tests for the evaluation of the influence of cracks and different crack widths on chloride penetration. Next to the steady state tests, also non-steady-state migration was used as a method to evaluate chloride ingress in cracked concrete [Audenaert et al. 2009; Maes et al. 2013]. Migration tests are very useful since they can be performed very fast. However, these test methods force the penetration of chlorides in the concrete by application of an electrical field. Consequently, only the migration coefficient of the concrete and the general chloride penetration (by spraying $AgNO_3$ on split specimens) can be determined. To determine the chloride profile and exact chloride concentrations inside the concrete, it is necessary to perform a chloride diffusion test. This test requires much more time, but it describes better the real mechanism of chloride penetration.

Despite of the use of different test methods, all studies agree that cracks in concrete increase the penetration of chlorides and hence impair the durability of concrete structures. Clearly, it would be interesting to use the concept of self-healing concrete in order to prevent ingress of chloride through cracks without need of repair works. During the past decade, a lot of research has been done on the autonomous healing of cracks in cementitious materials. Different methods have already been explored and one of the promising approaches is the embedment of encapsulated healing agents inside concrete [Van Tittelboom et al. 2011]. Encapsulation based self-healing materials sequester a healing agent inside discrete capsules. When a crack appears, the capsules break and the healing agent flows into the crack. The efficiency of this type of crack healing against chloride ingress has been investigated once before by Maes et al. [2014]. In that work it was concluded that capsule based self-healing had a beneficial influence on the resistance against chloride diffusion, but only worked in approximately 67% of the cases.

In this research a more extensive study on autonomous crack healing of concrete with encapsulated polyurethane was conducted. Two types of cracks were used to evaluate self-healing: standardized artificial cracks introduced by thin metal plates and realistic cracks introduced by a splitting test. A crack width of 300 µm was chosen since the allowable crack width in traditional steel reinforced concrete structures ranges from 300 to 400 µm depending on the environmental class [NBN EN 1992-1-1]. This paper reports the efficiency of the autonomous healing of the different cracks in concrete after 7 weeks of exposure to 165 g/l NaCl solution.

MATERIALS AND METHODS

Healing agent. A one component polyurethane precursor, developed in the framework of another project (SHEcon), was used as healing agent. The precursor had a viscosity of 6700 mPas at 25°C and an NCO-content of 7%. The polyurethane precursor starts reacting when it is exposed to moist surroundings. When exposed to a normal environment (e.g. 60% relative humidity) the solidification process of the polyurethane takes about 24 hours.

Glass capsules. The healing agent needs to be encapsulated in order to embed it inside the concrete matrix. Cylindrical glass capsules were used to carry the healing agent, similar to the ones used in previous research [Van Tittelboom et al. 2011; Maes et al. 2014]. The capsules were cut from a borosilicate glass tube with an outer diameter of 3.35 mm and an inner diameter of 3 mm. The length of the capsules was 35 mm. The advantage of using glass as an encapsulation material is the brittleness. The capsules will easily break when the healing action needs to be triggered. Glass is also an inert material, so it will not be affected by the encapsulated material and it can resist the high alkaline environment of the cement matrix. However, due to the high brittleness, the capsules cannot be mixed into the concrete. Consequently, the capsules will have to be placed into the molds before casting.

When the glass capsules were cut to the desired length, they were sealed by a two component polymethylmethacrylate (PMMA) glue at one end. Then the polyurethane precursor was injected in the capsules by means of a syringe with a needle. Finally, the other ends of the capsules were also sealed with PMMA.

Concrete specimens. A fly ash containing concrete mix with a water-to-binder (W/B) ratio of 0.41 was made. A fly ash-to-binder (F/B) ratio of 15% was used, according to the k-value concept [NBN B15-001 2004]. Fly ash concrete was chosen because the resistance to chloride penetration is higher than for ordinary Portland cement concrete [Van den Heede 2014]. The concrete composition is given in Table 1.

Table 1. Concrete Mix Composition and Properties

	Fly ash concrete
Sand 0/4 (kg/m³)	696
Aggregates 2/8 (kg/m³)	502
Aggregates 8/16 (kg/m³)	654
CEM I 52.5 N (kg/m³)	317.6
Fly Ash (kg/m³)	56
Water (kg/m³)	153
Superplasticizer (ml/kg binder)	3.0
W/B (-)	0.41
F/B (%)	15
Slump	S3
Strength class	C40/50

Concrete cylinders with a diameter of 100 mm and a height of 50 mm were cast in cylindrical PVC molds. The molds were clamped on a wooden base and the concrete was compacted on a vibration table. After casting, all specimens were placed in an air-conditioned room with a temperature of 20 ± 2 °C and a relative humidity of at least 95% for 24 hours. The specimens were then demolded and stored under the same conditions until the age of 28 days.

In order to investigate chloride ingress in cracks in concrete and evaluate the efficiency of autonomous crack healing, two types of cracks were introduced in the concrete specimens: standardized artificial cracks and realistic cracks. For both crack types, a target crack width of 300 µm was chosen since most design codes limit the crack width to this value.

This means that a total of five different series of concrete cylinders were made: uncracked specimens, specimens containing an artificial crack, specimens containing an artificial self-healing crack, specimens

with a realistic crack and specimens with a realistic self-healing crack. For each series, three specimens were made.

Specimens with artificial (self-healing) cracks. Artificial cracks were produced by introducing thin brass plates with a thickness of 300 µm into the fresh concrete. The thin plates were positioned on iron rods in the center of the molds. The iron rods were fixed on the wooden base plate by magnetic bases. When all plates were positioned, the concrete was poured into the molds and compacted by vibration. 24 hours after casting, the brass plates were carefully removed, creating artificial cracks with a length of 60 mm and a depth of 25 mm.

For autonomous crack healing, capsules embedded in the concrete matrix need to break at the moment of crack appearance. A method as described by Van Belleghem et al. 2015 was used to introduce an autonomous crack healing mechanism for artificial cracks. Three holes with a diameter of 3.5 mm were drilled in the thin brass plates. Capsules filled with healing agent were then put through these holes and glued on nylon threads with PMMA to fix their position in the molds (Figure 1a). The intermediate distance between the capsules was 20 mm and they were fixed at a depth of 12.5 mm (half of the crack depth). When the specimens had reached the age of 28 days, the plates were pulled out of the concrete. The removal of the plates caused the capsules to break and triggered the healing mechanism.

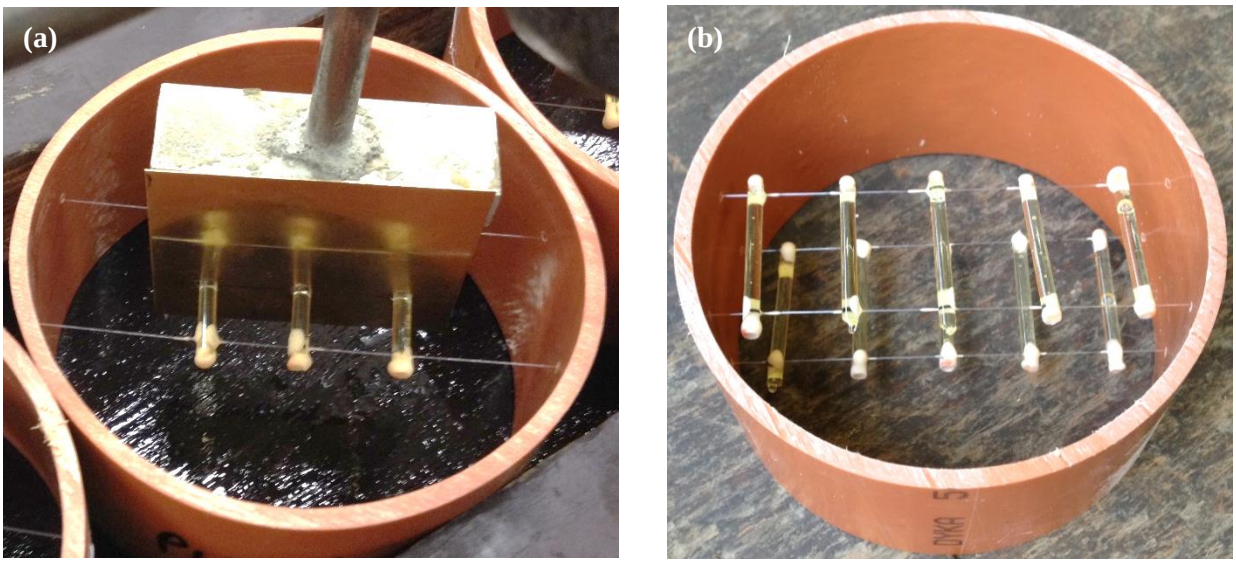

Figure 1. Specimens containing an autonomous crack healing mechanism for (a) artificial cracks and (b) realistic cracks

After all plates were removed from the specimens, the outermost layer (approximately 1 mm) of the test face of all specimens was cut off by water-cooled sawing. This was done to obtain a perfectly flat test surface. Finally, all sides of the specimens, except the test surface, were coated with a two component epoxy coating. This coating ensured that chlorides could only enter the concrete through the test surface.

Specimens with realistic (self-healing) cracks. To create realistic cracks, concrete cylinders were subjected to a crack width controlled splitting test at the age of 28 days. Before doing so, the outermost layer (approximately 1 mm) of both the upper and lower face of the cylinders was cut off by water-cooled sawing. Again, this was done to obtain flat surfaces at both sides of the cylinders. A Linear Variable Differential Transformer (LVDT) was attached to each side of the specimen at middle height to measure

the crack width during the splitting test. The crack width was increased with a velocity of 0.8 µm/s until a crack width of 600 µm was reached. During unloading, the crack width decreased to a final value between 100 and 400 µm.

The cracks created by the splitting test run through the whole diameter and over the complete height of the specimens. After crack creation, the crack width at both sides of the specimens was measured microscopically. Based on these measurements, it was decided which side of the specimen to use as testing surface. When the testing surface was selected, the other sides of the specimens were coated with epoxy coating.

In case of the self-healing specimens with realistic cracks, capsules filled with polyurethane precursor were fixed on nylon threads in the PVC molds (Figure 1b). In order to be able to compare the autonomous crack healing of artificial and real cracks, the amount of capsules and consequently the amount of healing agent available to seal the volume of the realistic cracks had to be the same as for the artificial cracks. Since the realistic cracks run through the whole diameter and height of the specimens, two rows of five capsules were placed in the molds. The spacing between the capsules in one row was 20 mm and the outer capsules were placed at 10 mm from the edge of the specimens. The two rows of capsules were fixed at a depth of 12.5 mm below the surface.

Crack width measurements. The crack width of all artificial and realistic cracks was measured microscopically on the surface of each specimen. A stereomicroscope, Leica S8 APO with DFC 295 camera, was used. Six images were taken along the length of the crack for artificial cracks. For realistic cracks, images were taken at nine points along the crack length. On each of the images the crack width was measured three times using the software ImageJ.

Chloride diffusion test. To evaluate the chloride ingress into the different specimens, an accelerated chloride diffusion test according to the standard NT Build 443 [1995] was performed. All coated specimens were immersed in an aqueous NaCl solution with a concentration of 165 g/l for 7 weeks. During the exposure, the temperature was kept constant at 20°C. After the exposure time of 7 weeks, layers with a thickness of 2 mm were ground off parallel to the exposed surface. A distinction was made between the chloride ingress in the zone of the crack and the chloride ingress in a zone further away from the crack. Therefore, the layers were ground off in two phases, similar to the method used by Maes et al. 2014. During the first phase, powder was collected in a zone of 16 x 78 mm around the crack. In the second phase, powder was collected further away from the crack in a circle with a diameter of 78 mm. The total chloride content of each powder was determined by means of acid-soluble chloride extraction in a nitric acid solution followed by a potentiometric titration against silver nitrate [Mu 2012].

RESULTS AND DISCUSSION

Crack width. The mean measured crack width of the artificial cracks was 297 ± 5 µm. Clearly, this agrees well to the thickness of the brass plates (300µm). The realistic cracks, induced by the splitting test, had a much larger deviation on the target crack width of 300 µm. Mean crack widths ranged from 110 to 396 µm. Since there were a large number of concrete cylinders subjected to the splitting test, the specimens with a mean crack width closest to 300 µm were chosen for investigation of the chloride diffusion. The mean crack width and standard error on the crack width of the chosen specimens are given in Table 2. For concrete containing the autonomous self-healing mechanism, less specimens were produced. It was found that the resulting crack width was also less than for the specimens without capsules. The mean crack width ranged from 139 to 219 µm. The values of the crack width of the self-healing specimens used for the chloride diffusion test are given in Table 2.

Table 2. Mean crack width of the specimens with realistic cracks

	Specimen	Mean crack width (µm)	Standard error (µm)
Reference concrete	A	300	22
	B	293	29
	C	298	24
Self-healing concrete	A	211	19
	B	219	17
	C	200	14

Effect of cracks on chloride penetration. Firstly, the effect of cracks on the ingress of chlorides is discussed. As mentioned before, quite a lot of research has already been done on this topic. Figure 2 shows the mean chloride profiles of uncracked samples and samples with an artificial or realistic crack. The left graph in the figure shows the chloride profiles of the zone directly around the crack, the right graph shows the chloride profiles of the zone next to the crack. All values in the graphs represent the mean values of three specimens and the error bars represent the standard errors on the mean values.

The left graph of Figure 2 clearly shows that both artificial and realistic cracks had a big influence on the penetration of chlorides. In the zone around the crack the chloride concentration was more or less constant at a depth of 14 – 20 mm for both uncracked and cracked concrete. The mean chloride concentration at this depth was 0.084 m%/binder for uncracked concrete. For concrete with an artificial or realistic crack this was 1.536 m%/binder or 1.683 m%/binder, respectively. Thus, the chloride concentration in the concrete at a depth higher than 14 mm, possibly at the location of the steel reinforcement, was 18 to 20 times higher due to the presence of a crack. These chloride concentrations are close to or even exceed the critical chloride content of reinforced concrete reported in literature [Angst et al. 2009; Sun et al. 2015]. However, the values of the chloride concentration found in this research are due to an accelerated chloride diffusion test. In reality, an exposure time longer than 7 weeks will be needed to reach these values. In any case it may be concluded that the risk for chloride-induced corrosion will be much higher when cracks are present.

When the chloride profiles of artificial and real cracks were compared, the results were quite similar from a depth of 8 mm onwards. Generally, it is pointed out in literature that artificial cracks do not predict the real behavior of chloride penetration or other aggressive substances since they do not include effects of tortuosity, connectivity and surface roughness of real cracks [Šavija and Schlangen 2010]. The similarity of the chloride profiles of both artificial and realistic cracks from a depth of 8 mm onwards shows that these effects were limited and artificial cracks were able to give a good approximation of the chloride ingress through cracks. However, it must be stated that a higher chloride concentration was detected around the artificial crack for the first layers (0 – 8 mm).

From the right graph in Figure 2 it can be seen that the mean chloride profile of concrete next to a crack was quite similar to uncracked concrete. This indicates that the penetration of chlorides perpendicular to the crack was very limited. From a depth of 10 mm, the chloride profile in the concrete next to the artificial crack was almost equal to uncracked concrete. It reached a more or less constant value of 0.103 m%/binder which was very similar to the value found for uncracked concrete. The concrete next to the realistic crack had a chloride profile with the same shape at a depth of 10 mm or higher, but the chloride content was always approximately 0.250 m%/binder higher. Apparently the chloride penetration perpendicular to the crack face was higher for realistic cracks at depths larger than 10 mm below the surface. The reason for this might be that the crack wall of a realistic crack was a rough surface instead of a cast surface, which might lead to a higher penetration of chlorides. It is also possible that the realistic

crack created by the splitting test did not run perfectly through the middle of the specimen, so part of the crack might be close to the area ground further away from the crack. Also, the presence of microcracks due to the loading of the specimens might be a reason for the slightly higher chloride concentration in the area further away from the crack.

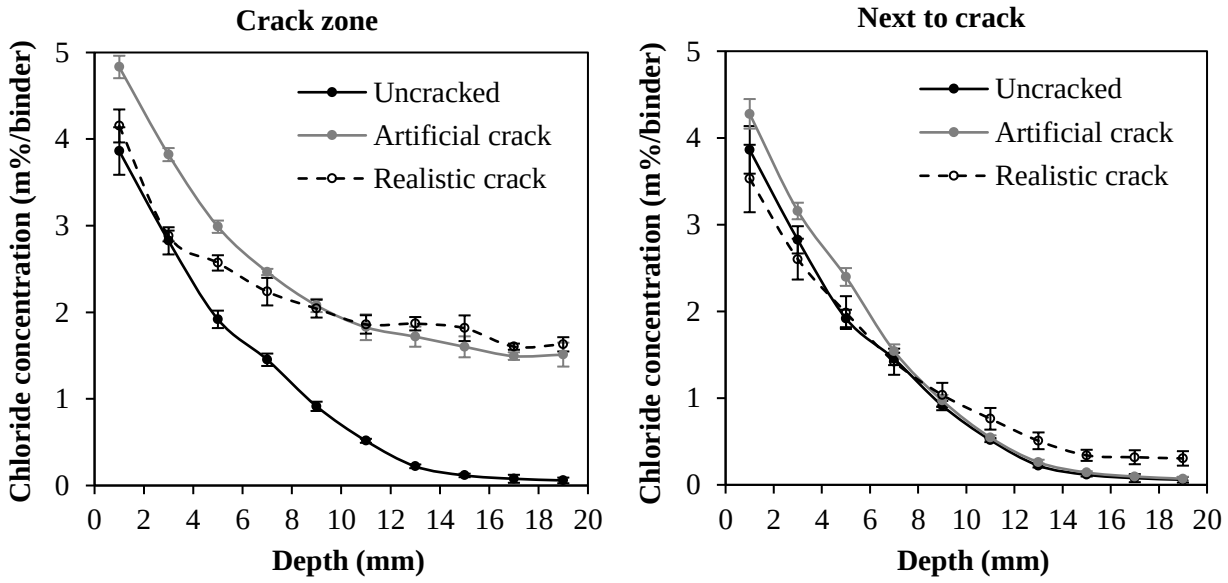

Figure 2. Average chloride profiles for uncracked concrete and concrete with artificial and realistic cracks in the zone around the crack (left) and in the zone next to the crack (right)

Resistance of autonomously healed concrete to chloride penetration. Figures 3 and 4 show the comparison between the mean chloride profiles in the crack zone and the zone next to the crack for cracked and healed concrete specimens. From the chloride profiles in the crack zones it is very clear that the healing of cracks with encapsulated polyurethane reduced the chloride concentration to a large extent, especially in the deeper layers. For both artificial and realistic cracks, crack healing reduced the chloride concentration in the top layers (0 – 6 mm) by 10 to 30%. In the layers at a depth of 14 – 20 mm the healing effect was even more visible, reducing the chloride concentration by 67 to 74%.

As mentioned in the previous section for cracked concrete, the chloride concentration was more or less constant at a depth of 14 mm or higher. For artificial healed cracks this concentration was 0.426 m%/binder. Compared to the concentration of an unhealed crack (1.536 m%/binder), this resulted in a mean reduction of the chloride concentration of 72%. In case of realistic healed cracks a mean concentration of 0.546 m% binder was found in the layers at a depth of 14 mm or higher, which was a reduction of 68% compared to an unhealed crack. Since the mean chloride concentration of healed concrete in the crack zone was still higher than the value found for uncracked concrete, some chlorides may still penetrate through the crack. However, crack healing formed a good partial barrier which prevented the immediate ingress of chloride ions through the crack. The chloride concentration at the location of the reinforcing steel will be much lower, reducing the chance of reaching the critical value. In this way, the time to corrosion initiation will be higher and the lifetime of the structure will be extended.

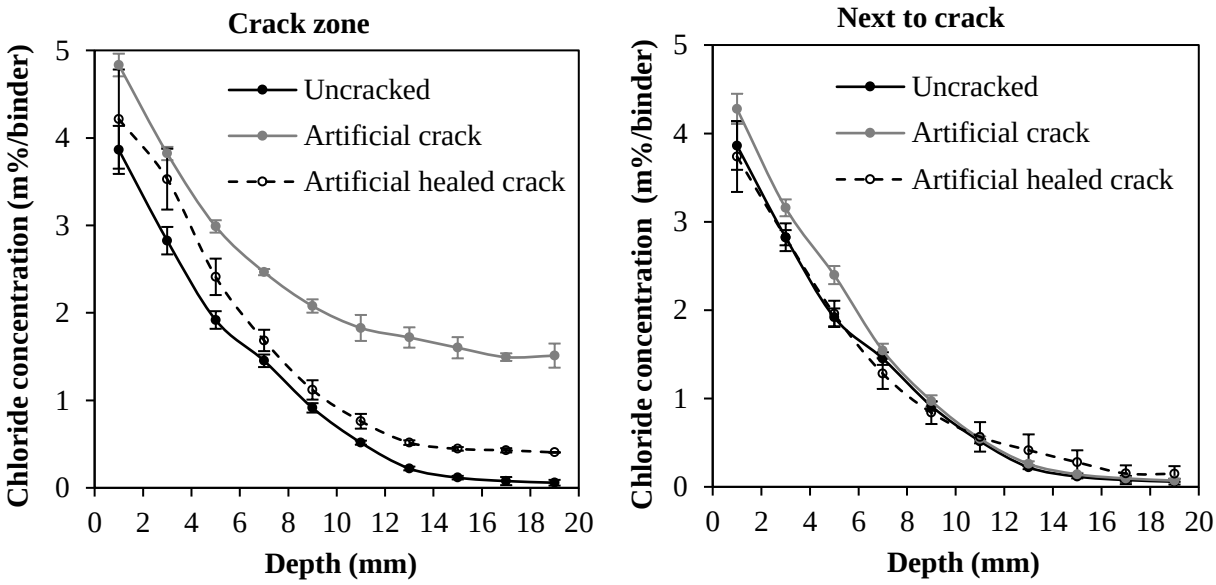

Figure 3. Comparison of the average chloride profiles for artificially cracked and healed concrete in the zone around the crack (left) and in the zone next to the crack (right)

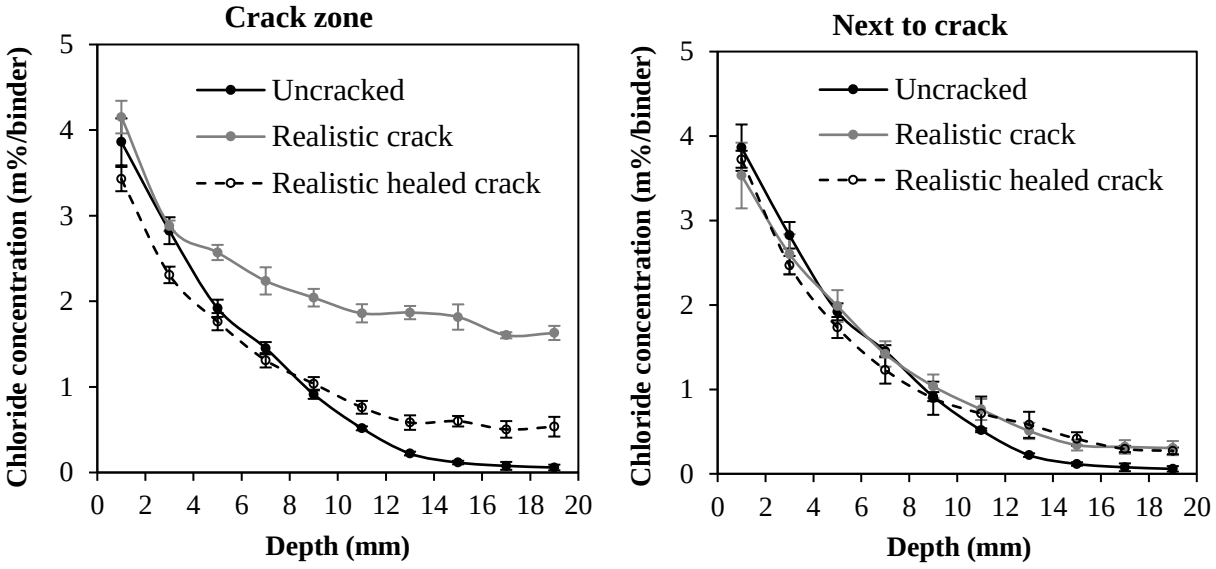

Figure 4. Comparison of the average chloride profiles for cracked and healed concrete with realistic cracks in the zone around the crack (left) and in the zone next to the crack (right)

The graphs on the right side in Figures 3 and 4 indicate that all specimens containing (healed) cracks had a chloride profile next to the crack which was very similar to uncracked concrete. As already mentioned, the chloride concentration next to the realistic cracks at a depth higher than 10 mm was slightly higher than for uncracked concrete. For realistic healed cracks the same was noticed, which means that crack healing was not able to reduce the chloride concentration in the zone next to the cracks. Since there was a

very clear healing effect in the crack zone, the higher chloride concentration in the zone next to the cracks must be attributed to the presence of microcracks or to the fact that the cracks do not run perfectly through the middle of the specimen, rather than penetration of chlorides perpendicular to the crack wall.

CONCLUSION

Cracks in concrete have a big influence on the penetration of chlorides. The chloride concentration in the concrete in a zone near to the crack was found to be much higher than for uncracked concrete. At a depth of 14-20 mm the chloride concentration of cracked and uncracked concrete was more or less constant. For cracked specimens this chloride concentration was 18 to 20 times higher than for uncracked samples. When steel reinforcement would be present at this depth, the critical chloride content would locally be reached much faster due to the presence of a crack. Consequently, the time to corrosion initiation will drastically decrease.

When the chloride content in the concrete zone next to the crack was analyzed, it was seen that the chloride profile was very similar to uncracked concrete. The chloride concentration in concrete next to an artificial crack at depths higher than 14 mm was 0.103 m%/binder, which was indeed very close to the value for uncracked concrete. When a real crack was present, the chloride concentration was somewhat higher, up to 0.320 m%/binder. Since these chloride concentrations were still quite low, it can be concluded that the chloride penetration perpendicular to the crack face was limited.

Autonomous healing of cracks by means of embedded capsules filled with polyurethane proved to be a very efficient technique to prevent chloride ingress into cracks. In the top layers (0 – 6 mm) of the concrete, a reduction of the chloride concentration of 10 – 30% was found due to crack healing. The chloride concentration in the layers at a depth of 14 – 20 mm could be reduced up to 74%. Crack healing thus forms a partial barrier which prevents the immediate ingress of chlorides to the steel reinforcement. This can prolong the time to rebar corrosion, since the chloride concentration at the depth of the steel rebar will be much lower. Consequently, crack healing can prolong the service life of concrete structures.

Further research will be conducted to investigate to what extent the crack healing by polyurethane is able to reduce the chloride concentration when the exposure time to chlorides is longer than 7 weeks. Therefore, chloride diffusion tests will be conducted on cracked and healed concrete specimens exposed to chlorides for 19 and 52 weeks. Also, a different type of polyurethane which has a lower viscosity will be tested. A less viscous healing agent might be able to fill the crack even more, which might lead to an even bigger reduction of the chloride ingress.

ACKNOWLEDGEMENTS

This research, performed under the program SHE (Engineered Self-Healing materials) (project ISHECO: Impact of Self-Healing Engineered Materials on steel COrrosion of reinforced concrete), was funded by SIM (Strategic Initiative Materials in Flanders). The financial support from the foundation for this study is gratefully acknowledged.

REFERENCES

Angst, U., Elsener, B., Larsen, C.K. and Vennesland, O. (2009). “Critical chloride content in reinforced concrete – A review.” *Cement and Concrete Research*, 39(12), 1122-1138.

Audenaert, K., De Schutter, G. and Marsavina, L. (2009). "Influence of cracks and crack width on penetration depth of chlorides in concrete." European Journal of Environmental and Civil Engineering, 13(5), 561-572.

Djerbi, A., Bonnet, S., Khelidj, A. and Baroghel-bouny, V. (2008). "Influence of traversing crack on chloride diffusion into concrete." *Cement and Concrete Research*, 38(6), 877-883.

Jacobsen, S., Marchand, J. and Boisvert, L. (1996). "Effect of cracking and healing on chloride transport in OPC concrete." *Cement and Concrete Research*, 26(6), 869-881.

Jang, S.Y., Kim, B.S. and Oh, B.H. (2011). "Effect of crack width on chloride diffusion coefficients of concrete by steady-state migration tests." *Cement and Concrete Research*, 41(1), 9-19.

Maes, M., De Belie, N. (2013). "Resistance of cracked concrete to chloride attack." *Proceedings of 3rd International Conference on Sustainable Construction Materials & Technologies,* 1-10.

Maes, M., Van Tittelboom, K. and De Belie, N. (2014). "The efficiency of self-healing cementitious materials by means of encapsulated polyurethane in chloride containing environments." *Construction and Building Materials*, 71, 528-537.

Mu, S. (2012). Chloride penetration and service life prediction of cracked self-compacting concrete, PhD thesis, Ghent University, Faculty of Engineering and Architecture. Ghent, Belgium.

NBN B15-001 (2004). Supplement to NBN EN 206-1: "Concrete – Specification, performance, production and conformity." Brussels: BIN, 27 pages.

NBN EN 1992-1-1 (2010). "Eurocode 2: Design of concrete structures. Part 1-1: General rules and rules for buildings. Brussels, Belgium: European Committee for Standardization, 238 pages.

NT Build 443 (1995). "Accelerated chloride penetration. Concrete hardened." Espoo, Finland: NordTest, 5 pages.

Šavija, B. and Schlangen, E. (2010). "Chloride ingress in cracked concrete – a literature review." *Advances in Modeling Concrete Service Life: Proceedings of 4th International RILEM PhD Workshop*, 133-142.

Sun, C., Liu, S., Niu, J. and Xu, W. (2015). "Critical chloride concentration of rebar corrosion in fly ash concrete." *International Journal of Electrochemical Science*, 10(7), 5309-5326.

Van Belleghem, B., De Belie N., Dewanckele, J. and Cnudde, V. (2015). "Analysis and visualization of water uptake in cracked and healed mortar by water absorption tests and X-ray radiography." *Concrete Repair, Rehabilitation and Retrofitting IV: 4th International Conference on Concrete Repair, Rehabilitation and Retrofitting (ICCRRR-4)*, 45-53.

Van den Heede, P. (2014). "Durability and Sustainability of Concrete with High Volumes of Fly Ash." PhD thesis, Ghent University, Faculty of Engineering and Architecture. Ghent, Belgium.

Van Tittelboom, K., De Belie, N., Van Loo, D. and Jacobs, P. (2011). "Self-healing efficiency of cementitious materials containing tubular capsules filled with healing agent." *Cement and Concrete Composites*, 33(4), 497-505.